Alexandria Engineering Journal (2014) 53, 757–766

FACULTY OF ENGINEERING
ALEXANDRIA UNIVERSITY

Alexandria University

Alexandria Engineering Journal

www.elsevier.com/locate/aej
www.sciencedirect.com

ORIGINAL ARTICLE

Flow and heat transfer characteristics of nanofluids in a rotating frame

Kalidas Das *

Department of Mathematics, Kalyani Government Engineering College, Kalyani, Nadia, West Bengal 741235, India

Received 20 December ; revised 8 April 2014; accepted 15 April 2014
Available online 10 May 2014

KEYWORDS

Heat transfer;
Nanofluids;
Rotating frame;
Convective transport

Abstract The problem of unsteady MHD free convection flow of nanofluids via a porous medium bounded by a moving vertical semi-infinite permeable flat plate with constant heat source and convective boundary condition in a rotating frame of reference is studied theoretically. The velocity along the plate i.e. slip velocity is assumed to oscillate in time with constant frequency so that the solutions of the boundary layer are the same oscillatory type. The dimensionless governing equations for this investigation are solved analytically using small perturbation approximation. Two types of nanofluids, namely Cu–water and Al_2O_3–water are used. The effects of various parameters on the flow and heat transfer characteristics are discussed through graphs and tables.

1. Introduction

Convective heat transfer in nanofluids is a topic of major contemporary interest both in sciences and in engineering. Heating or cooling fluids such as water, ethylene glycol and engine oil play a crucial role in thermal management of high tech industries but they have poor thermal characteristics, in particular thermal conductivity. Despite the considerable efforts to improve the rate of heat transfer by the usage of extended surfaces, mini-channels and microchannels, further enhancement in heating and cooling rate is always in demand. As solid materials possess higher thermal conductivities many studies have been carried out on thermal properties of suspension of solid particles in conventional heat transfer fluids. Nanotechnology provides means to manufacture solid particles in nanometer scale. Choi [1] was the first to introduce the word nanofluid that represents the fluid in which nanoscale particles (diameter less than 50 nm) are suspended in the base fluid. Nanoparticles are of great scientific interest as they are effectively a bridge between bulk materials and atomic or molecular structures. The common nanoparticles that have been used are aluminum, copper, iron and titanium or their oxides. Experimental studies [2–5] show that even with the small volumetric fraction of nanoparticles (usually less than 5%), the thermal conductivity of the base liquid can be enhanced by 5–20%. The enhanced thermal conductivity of nanofluid together with the thermal conductivity of the base liquid and turbulence induced by their motion contributes to a remarkable improvement in the convective heat transfer coefficient. This feature of nanofluids makes them attractive for the use in application such as advanced nuclear system [6]. Various benefits of the

* Tel.: +91 9748603199.
E-mail address: kd_kgec@rediffmail.com
Peer review under responsibility of Faculty of Engineering, Alexandria University.

ELSEVIER Production and hosting by Elsevier

1110-0168 © 2014 Production and hosting by Elsevier B.V. on behalf of Faculty of Engineering, Alexandria University.
http://dx.doi.org/10.1016/j.aej.2014.04.003

application of nanofluids include the following: improved heat transfer, heat transfer system size reduction, minimal clogging, micro-channel cooling and miniaturization of the system. Convective flow in porous media has been widely studied in the recent years due to its wide applications in engineering as post-accidental heat removal in nuclear reactors, solar collectors, drying processes, heat exchangers, geothermal and oil recovery, building construction etc. They are also used in other electronic applications which use microfluidic applications. It should be noticed that there have been published several recent papers [7–12] on the mathematical and numerical modeling of convective heat transfer in nanofluids. These models have some advantages over experimental studies due to many factors that influence nanofluid properties.

The problem on natural convection heat transfer in nanofluids has been investigated numerically by Gilles et al. [13], Jou and Tzeng [14], Ho et al. [15,16], Congedo et al. [17] and Ghasemi and Aminossadati [18]. However, the number of analytical studies on natural convection in nanofluids is relatively small compared with those devoted to forced convection. Khanafer et al. [19] analyzed the two dimensional natural convection flow of a nanofluid in an enclosure and found that for any given Grashof number, the heat transfer rate increased as the volume fraction of nanoparticles increased. Kim et al. [20] introduced a new friction factor to describe the effect of nanoparticles on the convective instability and the heat transfer characteristics of the base fluid. On the other hand, very few works have been done on natural convection flow of rotating fluids. Rotating flows of MHD non-Newtonian fluids have many applications in meteorology, geophysics, turbo machinery and many other fields. Such flows in the presence of a magnetic field are significant because of their geophysical and astrophysical importance. Moreover the present model has applications in biomedical engineering, for instance in the dialysis of blood in artificial kidney, blood flow in the capillaries, flow in blood oxygenation. Engineering applications include the design of filters, the porous pipe design, in transpiration cooling. Bakr [21] and Das [22] discussed free convection flow of micropolar fluid in a rotating frame of reference. Recently, Hamad and Pop [24] studied MHD free convection flow in a rotating frame of reference with constant heat source in a nanofluid. To develop the problem, they used the nanofluid model proposed by Tiwari and Das [23]. It is worth mentioning that while modeling the boundary layer flow and heat transfer, the boundary conditions that are usually applied are either a specified surface temperature or a specified surface heat flux. However, there are boundary layer flow and heat transfer problems in which the surface heat transfer depends on the surface temperature. Perhaps the simplest case of this is when there is a linear relation between the surface heat transfer and surface temperature. This situation arises in conjugate heat transfer problems and when there is Newtonian heating of the convective fluid from the surface. The situation with Newtonian heating arises in what is usually termed as conjugate convective flow, where the heat is supplied to the convective fluid through a bounding surface with a finite heat capacity. This results in the heat transfer rate through the surface being proportional to the local difference in the temperature with the ambient conditions. This configuration of Newtonian heating occurs in many important engineering devices, for example, in heat exchangers, where the conduction in a solid tube wall is greatly influenced by the convection in the fluid flowing over it. On the other hand, most recently, heat transfer problems for boundary layer flow concerning with a convective boundary condition were investigated by Aziz [25], Makinde and Aziz [26], Ishak [27] and Yacob et al. [28]. But so far, no attempt has been made to analyze the boundary layer flow of a nanofluid past a porous vertical moving plate in a rotating frame of reference with convective surface boundary condition.

The objective of the present study is to analyze the development of the unsteady free convection flow of a nanofluid past a moving vertical permeable flat plate in a rotating frame of reference with convective surface boundary condition. It is assumed that the plate is embedded in a uniform porous medium and oscillates in time with a constant frequency in the presence of a transverse magnetic field. The governing equations are solved analytically using perturbation technique. Numerical results are reported for various values of the physical parameters of interest. The organization of the paper is given as follows. The Section 2 deals with the mathematical formulation of the problems. Section 3 contains the closed form solutions of velocity and temperature. Numerical results and discussion are presented in Section 4. The conclusions have been summarized in Section 5.

2. Mathematical formulation of the problem

Consider the unsteady three dimensional free convection flow of an electrically conducting incompressible nanofluid of ambient temperature T_∞ past a semi-infinite vertical permeable moving plate embedded in a uniform porous medium in the presence of thermal buoyancy effect with constant heat source and convective boundary condition. The fluid is a water based nanofluid containing two types of nanoparticles, either Cu (copper) or Al_2O_3 (aluminum oxide). The nanoparticles are assumed to have a uniform shape and size. Moreover, it is assumed that both the fluid phase and nanoparticles are in thermal equilibrium state. Fig. 1 describes the physical model and the co-ordinate system. The flow is assumed to be in the x-direction which is taken along the plate in the upward direction and z-axis is normal to it. Also it is assumed that the whole system is rotate with a constant velocity Ω about z-axis. A uniform external magnetic field B_0 is taken to be acting along the z-axis. It is assumed that there is no applied voltage

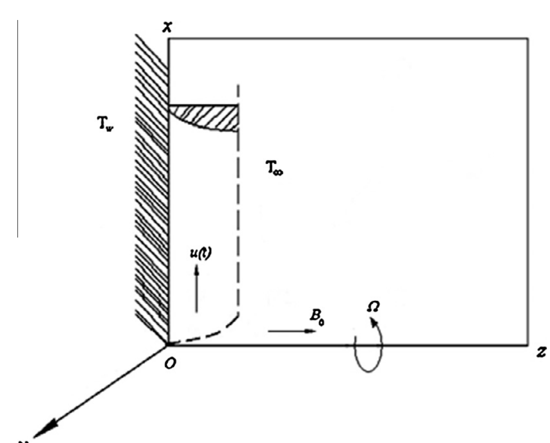

Figure 1 Physical model and coordinate system of the problem.

which implies the absence of an electric field. Also it is assumed that the induced magnetic field is small compared to the external magnetic field. This implies a small magnetic Reynolds number for the oscillating plate (see Liron and Wilhelm [29]). Due to semi-infinite plate surface assumption, furthermore, the flow variables are functions of z and time t only.

Under the boundary layer approximations, the basic equations that describe the physical situation are given by

$$\frac{\partial w}{\partial z} = 0 \tag{1}$$

$$\frac{\partial u}{\partial t} + w\frac{\partial u}{\partial z} - 2\Omega v = \frac{1}{\rho_{nf}}\left[\mu_{nf}\frac{\partial^2 u}{\partial z^2} + (\rho\beta)_{nf}g(T - T_\infty) - \frac{\mu_{nf}u}{k} - \sigma B_0^2 u\right] \tag{2}$$

$$\frac{\partial v}{\partial t} + w\frac{\partial v}{\partial z} + 2\Omega u = \frac{1}{\rho_{nf}}\left[\mu_{nf}\frac{\partial^2 v}{\partial z^2} - \frac{\mu_{nf}v}{k} - \sigma B_0^2 v\right] \tag{3}$$

$$\frac{\partial T}{\partial t} + w\frac{\partial T}{\partial z} = \alpha_{nf}\frac{\partial^2 T}{\partial z^2} - \frac{Q}{(\rho C_p)_{nf}}(T - T_\infty) \tag{4}$$

where u, v and w are velocity components along x, y and z-axis respectively, β_{nf} is the coefficient of thermal expansion of nanofluid, σ is the electric conductivity of the fluid, ρ_{nf} is the density of the nanofluid, μ_{nf} is the viscosity of the nanofluid, $(\rho C_p)_{nf}$ is the heat capacitance of the nanofluid, g is the acceleration due to gravity, k is the permeability of porous medium, T is the temperature of the nanofluid, Q is the temperature dependent volumetric rate of heat source, and α_{nf} is the thermal diffusivity of the nanofluid.

Further, we assume that the plate surface temperature is maintained by convective heat transfer at a certain value T_w (see [25–28]) which is to be determined later. Thus the boundary conditions are given by

$$u = v = 0, \quad T = T_\infty \text{ for } t \le 0 \tag{5}$$

$$\left.\begin{array}{l} u = U_r\left[1 + \frac{\varepsilon}{2}\{\exp(\mathrm{int}) + \exp(-\mathrm{int})\}\right], \quad v = 0, \quad -\kappa_{nf}\frac{\partial T}{\partial z} = h_f(T_w - T_\infty) \quad \text{at } z = 0 \\ \text{and} \\ u \to 0, \quad v \to 0, \quad T \to T_\infty \text{ as } z \to \infty \end{array}\right\}\text{for } t > 0 \tag{6}$$

where U_r is the uniform reference velocity and ε is the small constant quantity. The oscillatory plate velocity assumed in Eq. (6) is based on the suggestion proposed by Ganapathy [30].

The effective density of the nanofluid is given by

$$\rho_{nf} = (1 - \phi)\rho_f + \phi\rho_s \tag{7}$$

where ϕ is the solid volume fraction of nanoparticles. Thermal diffusivity of the nanofluid is

$$\alpha_{nf} = \frac{\kappa_{nf}}{(\rho C_p)_{nf}} \tag{8}$$

where the heat capacitance C_p of the nanofluid is obtained as

$$(\rho C_p)_{nf} = (1 - \phi)(\rho C_p)_f + \phi(\rho C_p)_s \tag{9}$$

and the thermal conductivity of the nanofluid κ_{nf} for spherical nanoparticles can be written as Maxwell [31]

$$\frac{\kappa_{nf}}{\kappa_f} = \frac{(\kappa_s + 2\kappa_f) - 2\phi(\kappa_f - \kappa_s)}{(\kappa_s + 2\kappa_f) + \phi(\kappa_f - \kappa_s)} \tag{10}$$

The thermal expansion coefficient of the nanofluid can be determined by

$$(\rho\beta)_{nf} = (1 - \phi)(\rho\beta)_f + \phi(\rho\beta)_s \tag{11}$$

Also the effective dynamic viscosity of the nanofluid given by Brinkman [32] as

$$\mu_{nf} = \frac{\mu_f}{(1 - \phi)^{2.5}} \tag{12}$$

where the subscripts nf, f and s represent the thermophysical properties of the nanofluids, base fluid and the nanosolid particles respectively and ϕ is the solid volume fraction of the nanoparticles. The thermophysical properties of the nanofluids are given in Table 1 (see Oztop and Abu-Nada [33]).

The continuity Eq. (1) gives

$$w = -w_0 \tag{13}$$

where the w_0 represents the normal velocity at the plate which is positive for suction and negative for injection.

Let us introduce the following dimensionless variables:

$$u' = \frac{u}{U_r}, \quad v' = \frac{v}{U_r}, \quad z = \frac{zU_r}{\nu_f}, \quad t' = \frac{tU_r^2}{\nu_f}, \quad n' = \frac{n\nu_f}{U_r^2}, \quad \theta = \frac{(T - T_\infty)}{(T_w - T_\infty)} \tag{14}$$

where ν_f is the kinematic viscosity of nanofluid. Then substituting Eq. (14) into Eqs. (2)–(4) yields the following dimensionless equations (dropping primes):

$$\left[1 - \phi + \phi\left(\frac{\rho_s}{\rho_f}\right)\right]\left(\frac{\partial u}{\partial t} - S\frac{\partial u}{\partial z} - Rv\right) = \frac{1}{(1-\phi)^{2.5}}\frac{\partial^2 u}{\partial z^2} + \left[1 - \phi + \phi\left(\frac{(\rho\beta)_s}{(\rho\beta)_f}\right)\right]\theta - \left(M^2 + \frac{1}{K}\right)u, \tag{15}$$

$$\left[1 - \phi + \phi\left(\frac{\rho_s}{\rho_f}\right)\right]\left(\frac{\partial v}{\partial t} - S\frac{\partial v}{\partial z} + Ru\right) = \frac{1}{(1-\phi)^{2.5}}\frac{\partial^2 v}{\partial z^2} - \left(M^2 + \frac{1}{K}\right)v, \tag{16}$$

Table 1 Thermophysical properties of regular fluid and nanoparticles.

Physical properties	Regular fluid (water)	Cu	Al_2O_3
C_p (J/kg K)	4179	385	765
ρ (kg/m^3)	997.1	8933	3970
κ (W/mK)	0.613	400	46
$\alpha \times 10^7$ (m^2/s)	1.47	1163.1	131.7
$\beta \times 10^{-5}$ (1/K)	21	1.67	0.63

$$\left[1-\phi+\phi\left(\frac{(\rho C_p)_s}{(\rho C_p)_f}\right)\right]\left(\frac{\partial\theta}{\partial t}-S\frac{\partial\theta}{\partial z}\right)=\frac{1}{\Pr}\left(\frac{\kappa_{nf}}{\kappa_f}\frac{\partial^2\theta}{\partial t^2}-Q_H\theta\right) \tag{17}$$

where $R=\frac{2\Omega\nu_f}{U_r^2}$ is the rotational parameter, $M=\frac{B_0}{U_r}\sqrt{\frac{\sigma\nu_f}{\rho_f}}$ is the magnetic field parameter, $\Pr=\frac{\nu_f}{\alpha_f}$ is the Prandtl number, $S=\frac{w_0}{U_r}$ is the suction ($S>0$) or injection ($S<0$) parameter, $K=\frac{kU_r^2}{\nu_f^2}$ is the permeability of the porous medium and $Q_H=\frac{Q\nu_f^2}{U_r^2\kappa_f}$ is the heat source parameter. The velocity characteristic U_r is defined as (Hamad and Pop [24]).

$$U_r=\left[g\beta_f(T_w-T_\infty)\nu_f\right]^{1/3}$$

Also the boundary conditions become

$$u=v=0,\quad \theta=0,\quad \text{for } t\le 0, \tag{18}$$

$$\left.\begin{array}{l} u=\left[1+\frac{\varepsilon}{2}\{\exp(\mathrm{int})+\exp(-\mathrm{int})\}\right],\quad v=0,\quad \theta'(0)=-\gamma[1-\theta(0)] \text{ at } z=0\\ \text{and}\\ u\to 0,\quad v\to 0,\quad \theta\to 0 \text{ as } z\to\infty \end{array}\right\}\text{for } t>0 \tag{19}$$

Here $\lambda=\frac{h_f\nu_f}{\kappa_f U_r}$ is the convective parameter. We now simplify Eqs. (15) and (16) by putting the fluid velocity in the complex form as

$V=u+iv$ and get

$$\left[1-\phi+\phi\left(\frac{\rho_s}{\rho_f}\right)\right]\left(\frac{\partial V}{\partial t}-S\frac{\partial V}{\partial z}+iRV\right)=\frac{1}{(1-\phi)^{2.5}}\frac{\partial^2 V}{\partial z^2}+\left[1-\phi+\phi\left(\frac{(\rho\beta)_s}{(\rho\beta)_f}\right)\theta-\left(M^2+\frac{1}{K}\right)V\right] \tag{20}$$

The associated boundary conditions (18) and (19) are written as follows:

$$V=0,\quad \theta=0,\quad \text{for } t\le 0, \tag{21}$$

$$\left.\begin{array}{l} V(0)=1+\frac{\varepsilon}{2}\{\exp(\mathrm{int})+\exp(-\mathrm{int})\},\quad \theta'(0)=-\gamma[1-\theta(0)]\\ V\to 0,\quad \theta\to 0, \text{ as } z\to\infty \end{array}\right\}$$
$$\text{for } t>0 \tag{22}$$

3. Analytical solutions

To find the analytical solutions of the system of partial differential Eqs. (17), (20) in the neighborhood of the plate under the boundary conditions (21), (22), we express V and θ as (see Ganapathy [30])

$$V(z,t)=V_0+\frac{\varepsilon}{2}[\exp(\mathrm{int})V_1(z)+\exp(-\mathrm{int})V_2(z)] \tag{23}$$

$$\theta(z,t)=\theta_0+\frac{\varepsilon}{2}[\exp(\mathrm{int})\theta_1(z)+\exp(-\mathrm{int})\theta_2(z)] \tag{24}$$

for ε (1). Invoking the above Eqs. (23) and (24) into the Eqs. (17), (20) and equating the harmonic and non-harmonic terms and neglecting the higher order terms of ε^2, we obtain the following set of equations:

$$\frac{1}{(1-\phi)^{2.5}}V''_0+S\left[1-\phi+\phi\left(\frac{\rho_s}{\rho_f}\right)\right]V'_0-\left[iR\left\{1-\phi+\phi\left(\frac{\rho_s}{\rho_f}\right)\right\}+M^2+\frac{1}{K}\right]V_0+\left[1-\phi+\phi\left(\frac{(\rho\beta)_s}{(\rho\beta)_f}\right)\right]\theta_0=0 \tag{25}$$

$$\frac{1}{(1-\phi)^{2.5}}V''_1+S\left[1-\phi+\phi\left(\frac{\rho_s}{\rho_f}\right)\right]V'_1-\left[i(R+n)\left\{1-\phi+\phi\left(\frac{\rho_s}{\rho_f}\right)\right\}+M^2+\frac{1}{K}\right]V_1+\left[1-\phi+\phi\left(\frac{(\rho\beta)_s}{(\rho\beta)_f}\right)\right]\theta_1=0 \tag{26}$$

$$\frac{1}{(1-\phi)^{2.5}}V''_2+S\left[1-\phi+\phi\left(\frac{\rho_s}{\rho_f}\right)\right]V'_2-\left[i(R-n)\left\{1-\phi+\phi\left(\frac{\rho_s}{\rho_f}\right)\right\}+M^2+\frac{1}{K}\right]V_2+\left[1-\phi+\phi\left(\frac{(\rho\beta)_s}{(\rho\beta)_f}\right)\right]\theta_2=0 \tag{27}$$

$$\frac{\kappa_{nf}}{\kappa_f}\theta''_0+\Pr\ S\left[1-\phi+\phi\left(\frac{(\rho C_p)_s}{(\rho C_p)_f}\right)\right]\theta'_0-Q_H\theta_0=0 \tag{28}$$

$$\frac{\kappa_{nf}}{\kappa_f}\theta''_1+\Pr\ S\left[1-\phi+\phi\left(\frac{(\rho C_p)_s}{(\rho C_p)_f}\right)\right]\theta'_1-\left[in\ \Pr\left\{1-\phi+\phi\left(\frac{(\rho C_p)_s}{(\rho C_p)_f}\right)\right\}+Q_H\right]\theta_1=0 \tag{29}$$

$$\frac{\kappa_{nf}}{\kappa_f}\theta''_2+\Pr S\left[1-\phi+\phi\left(\frac{(\rho C_p)_s}{(\rho C_p)_f}\right)\right]\theta'_2+\left[in\ \Pr\left\{1-\phi+\phi\left(\frac{(\rho C_p)_s}{(\rho C_p)_f}\right)\right\}-Q_H\right]\theta_2=0 \tag{30}$$

where the primes denote differentiation w.r.t z.

The corresponding boundary conditions can be written as

$$V_0=V_1=V_2=1,\quad \theta'_0=-\gamma[1-\theta_0],\quad \theta'_1=\gamma\theta_1,\quad \theta'_2=\gamma\theta_2 \text{ at } z=0 \tag{31}$$

$$V_0\to 0, V_1\to 0, V_2\to 0, \theta_0\to 0, \theta_1\to 0, \theta_2\to 0 \text{ as } z\to\infty \tag{32}$$

Solving Eqs. (25)–(30) under the boundary conditions (31), (32) we obtain the expression for velocity and temperature as

$$V=A_1\exp(-m_1z)+(1-A_1)\exp(-m_2z)+\frac{\varepsilon}{2}\{\exp(-m_3z+\mathrm{int})+\exp(-m_4z-\mathrm{int})\}, \tag{33}$$

$$\theta = \frac{\gamma}{m_1 + \gamma} \exp(-m_1 z) \tag{34}$$

where

$$A_1 = -\frac{\gamma(1-\phi)^{2.5}\left[1-\phi+\phi\left(\frac{(\rho\beta)_s}{(\rho\beta)_f}\right)\right]}{(m_1+\gamma)(m_1^2 - S_1 m_1 - B_1)},$$

$$m_1 = \frac{1}{2}\left[S_1 \mathrm{Pr}_1 + \sqrt{(S_1 \mathrm{Pr}_1)^2 + 4Q_H \frac{\kappa_f}{\kappa_{nf}}}\right],$$

$$m_j = \frac{1}{2}\left[S_1 + \sqrt{S_1^2 + 4B_{j-1}}\right], \quad j = 2, 3, 4$$

$$B_1 = M_1 + iR_1, \quad B_2 = M_1 + i(R_1 + n_1),$$
$$B_3 = M_1 + i(R_1 - n_1),$$

$$S_1 = S(1-\phi)^{2.5}\left[1-\phi+\phi\left(\frac{\rho_s}{\rho_f}\right)\right],$$

$$R_1 = R(1-\phi)^{2.5}\left[1-\phi+\phi\left(\frac{\rho_s}{\rho_f}\right)\right],$$

$$n_1 = n(1-\phi)^{2.5}\left[1-\phi+\phi\left(\frac{\rho_s}{\rho_f}\right)\right], M_1 = \left(M^2 + \frac{1}{K}\right)(1-\phi)^{2.5},$$

$$\mathrm{Pr}_1 = \frac{\mathrm{Pr}\kappa_f\left[1-\phi+\phi\left(\frac{(\rho C_p)_s}{(\rho C_p)_f}\right)\right]}{\kappa_{nf}(1-\phi)^{2.5}\left[1-\phi+\phi\left(\frac{\rho_s}{\rho_f}\right)\right]}$$

We notice that the solutions (33) and (34) approach to the solutions for the constant surface temperature as $\gamma \to \infty$. This can be seen from the boundary condition (22), which gives $\theta(0) = 1$ as $\gamma \to \infty$. Further, it is worth mentioning that Eqs. (33) and (34) reduce to those of Hamad and Pop [24] when $K \to \infty$ (non-porous medium) and $\gamma \to \infty$ (constant surface temperature).

The physical quantities of engineering interest are skin-friction coefficient C_f and the local Nusselt number Nu which are defined as

$$\begin{aligned} C_f &= \frac{(T_w)_{z=0}}{\rho_f U_r^2} = \frac{1}{(1-\phi)^{2.5}} V'(0) \\ &= -\frac{1}{(1-\phi)^{2.5}}\left[A_1 m_1 + (1-A_1)m_2 + \frac{\varepsilon}{2}\{m_3 \exp(\mathrm{int}) + m_4 \exp(-\mathrm{int})\}\right] \end{aligned} \tag{35}$$

and

$$Nu = -\frac{x\left(\frac{\partial T}{\partial z}\right)_{z=0}}{T_w - T_\infty} = -\frac{\kappa_{nf}}{\kappa_f} \mathrm{Re}_x \theta'(0) \tag{36}$$

where $\mathrm{Re}_x = \frac{U_r x}{\nu_f}$ is the local Reynolds number.

Thus

$$\frac{Nu}{\mathrm{Re}_x} = -\frac{\kappa_{nf}}{\kappa_f}\theta'(0) \tag{37}$$

4. Numerical results and discussion

In order to bring out the salient features of the flow and heat transfer characteristics with nanoparticles, the numerical results are presented in Figs. 2–10 and in Tables 2–5. In the numerical calculations we have used the data presented in Table 1 for the thermo-physical properties of the fluid and the nanoparticles (Cu, Al_2O_3). Following Oztop and Abu-Nada [33], we considered the range of nanoparticle volume fraction $0 \leqslant \phi \leqslant 0.2$. The Prandtl number Pr of the base fluid (water) is kept constant at 6.785. In the present study we have chosen $n = 10$, $nt = \frac{\pi}{2}$ and $\varepsilon = 0.02$ while ϕ, R, S, K, M, Q_H and γ are varied over a range, which are listed in the figures legends.

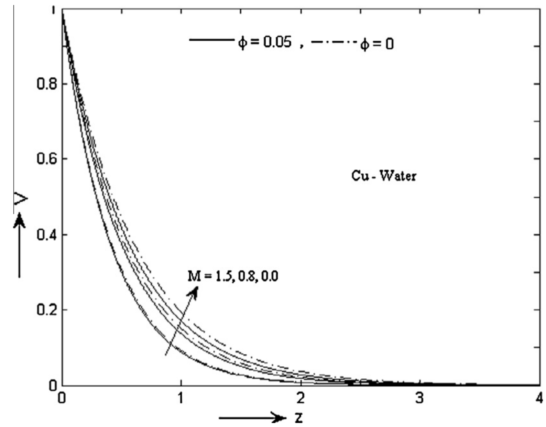

Figure 2 Velocity profiles for various values of M when $K = 1.0$, $S = 1$, $\gamma = 0.1$, $Q_H = 5$ and $R = 0.3$.

4.1. Effect of magnetic field parameter M

Fig. 2 illustrates the influence of the magnetic field parameter M on the velocity distribution for Cu–water nanofluid with $\phi = 0.0$ (regular fluid), 0.05 (nanofluid). It is clear from figures that the velocity distribution across the boundary layer reduces with an increase in the magnetic field parameter M and decreases asymptotically to zero at the edge of the hydrodynamic boundary layer. This yields a decrease in the boundary layer thickness. Thus hydrodynamic boundary layer thickness decreases as the magnetic field parameter M increases for both the regular and nanofluid and as a result, the local velocity also decreases. The reason behind this phenomenon is that application of magnetic field to an electrically conducting fluid gives rise to a resistive type force called the Lorentz force. This force has the tendency to slow down the motion of the fluid in the boundary layer. From Table 2, we observe that the skin friction coefficient C_f at the plate increases with an increase in the magnetic field parameter M at a specific permeability parameter K for both regular fluid and nanofluids. Also the skin friction coefficient for Cu–water solution is greater than for Al_2O_3–water solution. It is noticed that in the presence of nanoparticles the highest wall shear stress occurs. These observations show good agreement with the results of Hamad and Pop [24].

4.2. Effect of the permeability parameter K

For different values of the permeability parameter K, the velocity distribution on the porous wall is plotted in Fig. 3 for nanoparticle volume fraction $\phi = 0.0$ (regular fluid) and 0.1 (nanofluid) for Cu–water. It is obvious that the increased

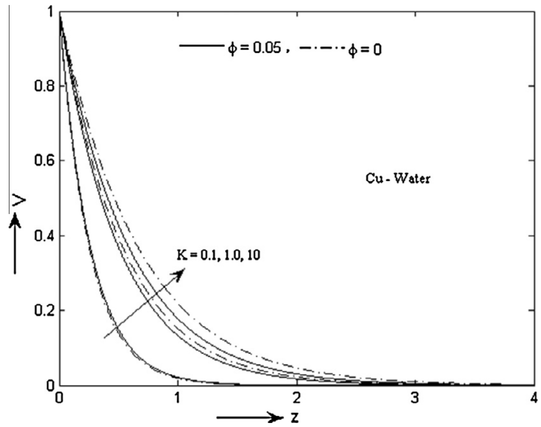

Figure 3 Velocity profiles for various values of K when $S = 1$, $M = 0.8$, $\gamma = 0.1$, $Q_H = 5$ and $R = 0.3$.

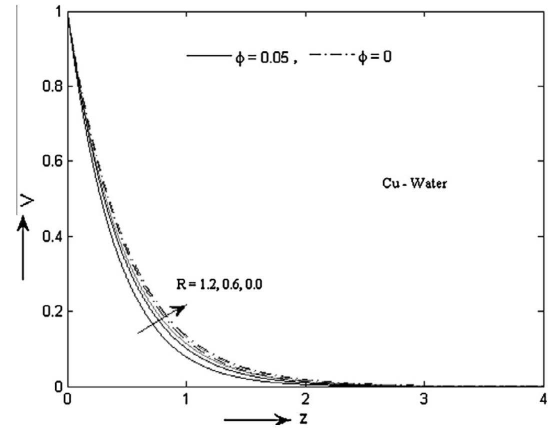

Figure 6 Velocity profiles for various values of R for $K = 1.0, S = 1$, $M = 0.8, \gamma = 0.1$ and $Q_H = 5$.

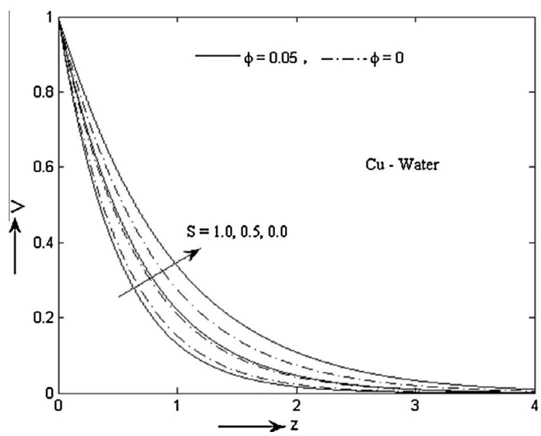

Figure 4 Velocity profiles for various values of S (>0) when $K = 1.0$, $M = 0.8$, $\gamma = 0.1$, $Q_H = 5$ and $R = 0.3$.

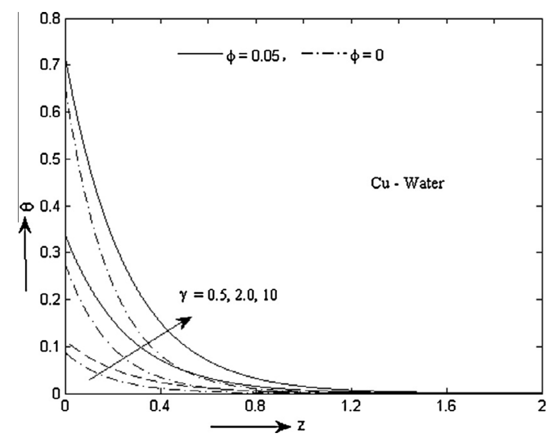

Figure 7 Temperature profiles for various values of γ when $K = 1.0$, $S = 1$, $M = 0.8$, $Q_H = 5$ and $R = 0.3$.

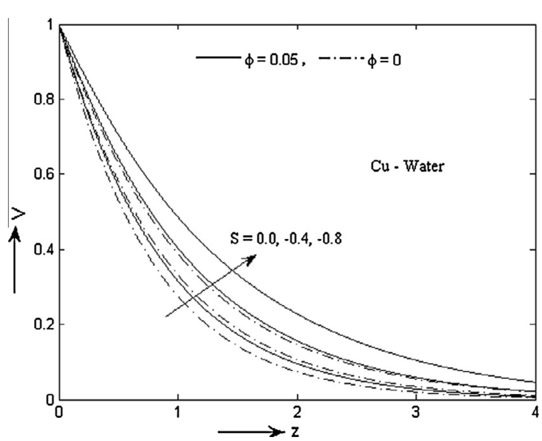

Figure 5 Velocity profiles for various values of S (<0) when $K = 1.0$, $M = 0.8$, $\gamma = 0.1$, $Q_H = 5$ and $R = 0.3$.

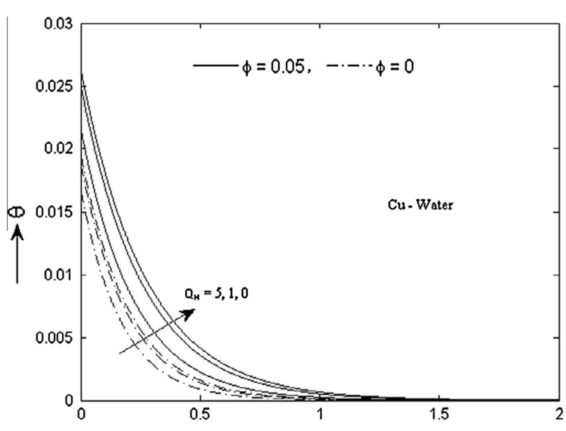

Figure 8 Temperature profiles for various values of Q_H when $K = 1.0$, $S = 1$, $M = 0.8$, $\gamma = 0.1$ and $R = 0.3$.

values of K tend to increasing of the velocity on the porous wall and so enhance the momentum boundary layer thickness. Table 3 shows the effect of the permeability parameter K on the skin friction coefficient C_f and the Nusselt number Nu/Re_x. It is seen that an increase in the permeability parameter K leads to a decrease in the skin friction coefficient for both nanofluids. Such effect is found to be more significant in the

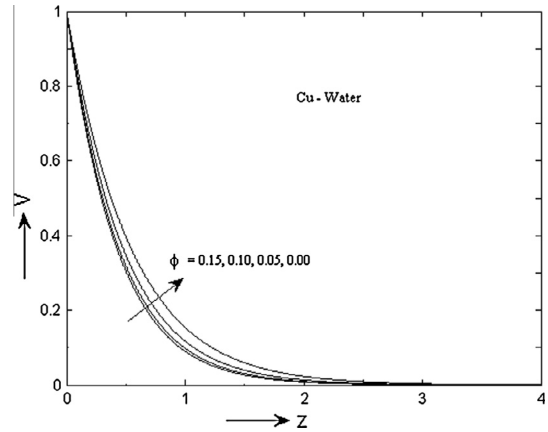

Figure 9 Velocity profiles for various values of ϕ when $K = 1.0$, $S = 1$, $M = 0.8$, $\gamma = 0.1$, $Q_H = 5$ and $R = 0.3$.

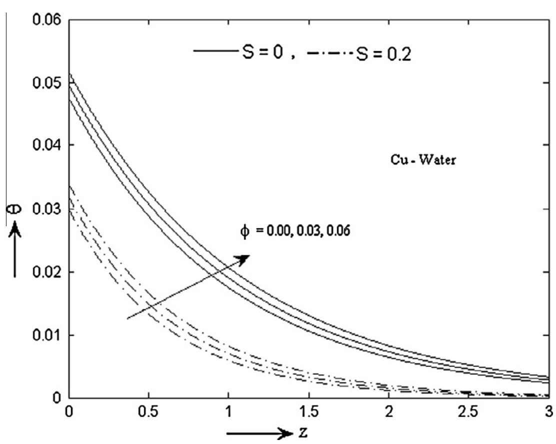

Figure 10 Temperature profiles for various values of ϕ when $K = 1.0$, $M = 0.8$, $\gamma = 0.1$, $Q_H = 5$ and $R = 0.3$.

Cu–water solution than in the Al_2O_3–water solution. But there is no effect of K on Nusselt number.

4.3. Effect of suction/injection parameter S

Figs. 4 and 5 demonstrate the effect of the suction/injection parameter S on the fluid velocity V for both regular fluid ($\phi = 0$) and nanofluid ($\phi = 0.1$). As an output of figures, it is understandable that the velocity of the fluid across the boundary layer decreases by increasing suction parameter $S\,(>0)$ whereas reverse effect occurs for injection parameter $S\,(<0)$ for both pure fluid and nanofluid with nanoparticles Cu. Also we see that as S increases, the velocity still approaches the same asymptotic value for large values of z. It is worth mentioning here that the influence of the suction and injection parameter S on the fluid velocity is more effective for nanofluid with nanoparticles Cu. Thus hydrodynamic boundary layer thickness decreases as the suction parameter $S\,(>0)$ increases for both the regular and nanofluids but the effect is opposite for injection parameter $S\,(<0)$. The influence of the suction/injection parameter S on the skin friction coefficient C_f and the Nusselt number Nu/Re_x are enlightened in Table 4. It is observed from this table that the shear stress at the wall increases with an increase in the suction parameter $S\,(>0)$ and effect is opposite for injection parameter $S\,(<0)$ for both regular fluid and nanofluid. It is worth mentioning that the presence of nanoparticles results in an increase in the shear stress. It is clear that the Nusselt number increases with the increase in suction parameter $S\,(>0)$ for both regular fluid and nanofluids with nanoparticles Cu and Al_2O_3 but the effect is reverse for injection parameter $S\,(<0)$. Another important fact is that the effect of S is more significant for nanofluid with nanoparticle Cu and Al_2O_3 than for regular fluid (water). This observations is in agreement with the results obtained by Hamad and Pop [24].

4.4. Effect of the rotational parameter R

The velocity profiles against z for different values of the rotational parameter R are displayed in Fig. 6 for both regular fluid ($\phi = 0$) and nanofluid ($\phi = 0.1$). It is observed that an increasing in R leads to decreasing in the values of the velocity across the boundary layer and so decrease the momentum boundary layer thickness. From Table 5 we show that as an

Table 2 Values of C_f and Nu/Re_x for different nanoparticles for various values of φ, M and γ.

φ	M	γ	Cu–Water		Al_2O_3–Water	
			C_f	Nu/Re_x	C_f	Nu/Re_x
0.0	0.0	0.1	1.9659	–	–	–
	0.5		2.0467	–	–	–
	1.0		2.2681	–	–	–
	1.5		2.5875	–	–	–
	0.5	0.5	2.0374	0.4644	–	–
		1.0	2.0293	0.8672	–	–
		5.0	1.9898	2.8320	–	–
		10.0	1.9674	3.9508	–	–
0.1	0.0	0.1	2.6970	–	2.3454	–
	0.5		2.7816	–	2.4357	–
	1.0		3.0167	–	2.6839	–
	1.5		3.3622	–	3.0438	–
	0.5	0.5	2.7672	0.6069	2.4225	0.6012
		1.0	2.7552	1.1150	2.4114	1.1048
		5.0	2.7015	3.3776	2.3620	3.3487
		10.0	2.6743	4.5255	2.3369	4.4882

Table 3 Values of C_f and Nu/Re_x for different nanoparticles for various values of φ, K and Q_H.

φ	K	Q_H	Cu–Water		Al_2O_3–Water	
			C_f	Nu/Re_x	C_f	Nu/Re_x
0.0	0.1	5.0	3.7125	–	–	–
	1.0		1.6935	–	–	–
	5.0		1.3232	–	–	–
	∞		1.2106	–	–	–
	0.5	0.0	2.0318	0.4545	–	–
		1.0	2.0327	0.4561	–	–
		3.0	2.0342	0.4586	–	–
		10.0	2.0374	0.4644	–	–
0.1	0.1	5.0	4.6094	–	4.3065	0.5939
	1.0		2.4186	–	2.0263	–
	5.0		2.0661	–	1.6257	–
	∞		1.9672	–	1.5087	0.5939
	0.5	0.0	2.7559	0.5864	2.4121	0.5808
		1.0	2.7581	0.5899	2.4141	0.5843
		3.0	2.7612	0.5953	2.4170	0.5897
		10.0	2.7672	0.6069	2.4225	0.6012

Table 4 Values of C_f and Nu/Re_x for different nanoparticles for various values of φ and S.

φ	S	Cu–Water		Al_2O_3–Water	
		C_f	Nu/Re_x	C_f	Nu/Re_x
0.0	0.0	1.4181	0.4086	–	–
	0.3	1.5930	0.4307	–	–
	0.6	1.7761	0.4467	–	–
	1.2	2.1720	0.4655	–	–
	−0.2	1.3065	0.3909	–	–
	−0.4	1.2000	0.3718	–	–
	−0.8	1.0081	0.3333	–	–
0.1	0.0	1.6114	0.5293	1.6142	0.5247
	0.3	1.9173	0.5573	1.8365	0.5523
	0.6	2.2586	0.5791	2.0753	0.5737
	1.2	3.0348	0.6070	2.6015	0.6012
	−0.2	1.4288	0.5076	1.4760	0.5034
	−0.4	1.2642	0.4845	1.3467	0.4807
	−0.8	0.9900	0.4378	1.1182	0.4348

increasing of the rotation parameter the skin friction coefficient increases for both nanofluid with nanoparticles Cu and Al_2O_3 but Nusselt number remain unchanged.

4.5. Effect of the convective parameter γ

Fig. 7 present typical profiles for temperature distribution for various values of the convective parameter γ for both regular and nanofluids with $\phi = 0.0$ (regular fluid), 0.1 (nanofluid). Figures indicate that temperature into the fluid field decreases on increasing γ in the boundary layer region and is maximum at the surface of the plate for both nanoparticles. Thus, by escalating γ, thermal boundary layer thickness enhances. So, we can interpret that the rate of heat transfer decreases with increase in convective parameter γ. This phenomenon is more prominent in the presence of nanofluid particle volume fraction ϕ. It should be noted that the solution approaches to the solution for constant surface temperature for large values of γ i.e. $\gamma \to \infty$. From the boundary condition (22), it can be seen that $\theta(0) = 1$ as $\gamma \to \infty$. These results are in agreement with the results obtained by Hamad and Pop [24]. The varia-

Table 5 Values of C_f and Nu/Re_x for different nanoparticles for various values of φ and R.

φ	R	Cu–Water		Al_2O_3–Water	
		C_f	Nu/Re_x	C_f	Nu/Re_x
0.00	0.3	2.0354	0.4607	2.0354	0.4607
0.04		2.3154	0.5134	2.1831	0.5114
0.08		2.6107	0.5698	2.3384	0.5655
0.12		2.9196	0.6303	2.5020	0.6233
0.14		3.0789	0.6622	2.5872	0.6537
0.05	0.0	2.3786	0.5271	2.2143	0.5271
	0.5	2.4040	–	2.2333	–
	1.5	2.5755	–	2.3666	–
	2.5	2.8235	0.5271	2.5695	0.5271

tion of the skin friction coefficient C_f and the Nusselt number Nu/Re_x with the convective parameter γ are shown in Table 2. Table shows that the skin friction coefficient C_f decreases as γ increases for both regular fluid and nanofluids with nanoparticles Cu and Al_2O_3. Also the Nusselt number increases with the increase in the convective parameter γ for nanofluids with nanoparticles Cu and Al_2O_3. The variation of Nu/Re_x is much more considerable for nanofluids. It is to be noted that highest heat transfer rate is obtained for Cu due to high thermal conductivity compared to Al_2O_3.

4.6. Effect of the heat generation parameter Q_H

Fig. 8 displays the temperature profiles for various values of the heat generation parameter Q_H for both regular fluid and nanofluids with nanoparticle Cu. The temperature in the boundary layer region decreases with the increase in the heat generation parameter Q_H and as a consequence the thermal boundary layer thickness decreases. These profiles satisfy the far field boundary conditions asymptotically, which support the numerical results obtained. Table 3 shows the effect of heat generation parameter Q_H on dimensionless shear stress (the skin friction coefficient) and heat transfer rate (Nusselt number) for both regular fluid and nanofluids. It is observed that the skin friction coefficient and Nusselt number both increase as Q_H increase for both regular fluid and nanofluids with nanoparticles Cu and Al_2O_3. These results is similar to that reported by Hamad and Pop [24].

4.7. Effect of nanoparticle volume fraction parameter ϕ

Fig. 9 illustrates the variation of the velocity distribution for various values of the nanoparticle volume fraction parameter ϕ. It is seen from these figures that the velocity distribution across the boundary layer decreases with the increase of ϕ. The influence of nanoparticle volume fraction parameter ϕ on the temperature are shown in Fig. 10 for Cu–water when $S = 0, 0.2$. It is seen from figures that the temperature profile increases with the increase in nanoparticle volume fraction parameter ϕ. Thus the thermal boundary layer thickness increases and tends asymptotically to zero as the distance increases from the boundary. From Table 5, one can be noted that the wall skin friction coefficient C_f increases with an increase in the nanoparticle volume fraction ϕ for both nanofluids. It is found from this table that for a particular nanoparticle, increasing nanoparticle volume fraction is to increase the heat transfer rate at the surface. Also the heat transfer rate for nanoparticles, namely Cu–water is greater than Al_2O_3–water. This is due to the high conductivity of the solid particles Cu than those of Al_2O_3. The presence of nanoparticles result in a increase in the Nusselt number Nu/Re_x. These results are found to be identical with the results of Hamad and Pop [24].

5. Conclusions

In this work, the effect of the metallic nanoparticles on unsteady MHD free convection flow and heat transfer of an incompressible conducting fluid along a semi-infinite vertical permeable moving plate embedded in a uniform porous medium in a rotating frame of reference have been studied. The main conclusions emerging from this study are as follows:

- In boundary layer region, the fluid velocity decreases with the increase in magnetic field parameter, suction parameter S, nanoparticle volume fraction and rotational parameter but effect is reverse for injection parameter and the permeability parameter.
- An increase in the convective parameter and nanoparticle volume fraction lead to increase the thermal boundary layer thickness but opposite effect occurs for heat generation parameter.
- The increasing values of γ, ϕ, Q_H and $S\ (>0)$ is to increase the numerical value of wall temperature gradient for both regular and nanofluids but effect is opposite for injection parameter $S\ (<0)$.
- The skin friction coefficient increases with the increase in the nanoparticle volume fraction, magnetic field parameter, suction parameter and rotational.

Acknowledgment

The author wish to express his cordial thanks to reviewers for valuable suggestions and comments to improve the presentation of this article.

References

[1] S.U.S. Choi, Enhancing thermal conductivity of fluids with nanoparticles, Devels Appls Non-Newtonian Flows 66 (1995) 99–105.
[2] H. Masuda, A. Ebata, K. Teramea, N. Hishinuma, Altering the thermal conductivity and viscosity of liquid by dispersing ultra-fine particles, Netsu Bussei 4 (4) (1993) 227–233.
[3] J.A. Eastman, S.L.S.S. Choi, W. Yu, L.J. Thompson, Anomalously increased effective thermal conductivity of ethylene glycol-based nanofluids containing copper nanoparticles, Appl. Phys. Lett. 78 (6) (2001) 718–720.
[4] Y. Xuan, Q. Li, Investigation on convective heat transfer and flow features of nanofluids, J. Heat Transf. 125 (2003) 151–155.
[5] .H.A. Minsta, G. Roy, C.T. Nguyen, D. Doucet, New temperature dependent thermal conductivity data for water-based nanofluids, Int. J. Ther. Sci. 48 (2009) 63–371.
[6] J. Buongiorno, L.W. Hu, Nanofluid Coolants for Advanced Nuclear Power Plants, Proceedings of ICAPP, Seoul, May 15–19 (2005).
[7] A.V. Kuznetsov, D.A. Nield, Natural convective boundary layer flow of a nanofluid past a vertical plate, Int. J. Ther. Sci. 49 (2010) 243–247.
[8] W.A. Khan, A. Aziz, Natural convection flow of a nanofluid over a vertical plate with uniform surface heat flux, Int. J. Ther. Sci. 50 (2011) 1207–1214.
[9] P.K. Kundu, K. Das, S. Jana, Nanofluid flow towards a convectively heated stretching surface with heat source/sink: a lie group analysis, Afr. Mat. (1012), doi 10.1007/s13370-012-0124-4.
[10] K. Das, Slip flow and convective heat transfer of nanofluids over a permeable stretching surface, Comput. Fluids 64 (2012) 34–42.
[11] K. Das, Lie group analysis for nanofluid flow past a convectively heated stretching surface, Appl. Math. Comput. 221 (2013) 547–557.
[12] K. Das, Nanofluid flow over a shrinking sheet with surface slip, Microfluid Nanofluid 16 (2014) 391–401.
[13] G.R. Gilles, C.T. Nguyen, P.R. Lajoie, Numerical investigation of laminar flow and heat transfer in a radial flow cooling system with the use of nanofluids, Super lattices Microstr. 35 (2004) 497–511.

[14] R.Y. Jou, S.C. Tzeng, Numerical research of nature convective heat transfer enhancement filled with nanofluids in rectangular enclosures, Int. Commun. Heat Mass Transf. 33 (2006) 727–736.

[15] C.J. Ho, M.W. Chen, Z.W. Li, Effect of natural convection heat transfer of nanofluid in an enclosure due to uncertainties of viscosity and thermal conductivity, in: Proceedings of ASME/JSME Thermal Engineering Summer Heat Transfer Conference-HT 1, (2007) 833–841.

[16] C.J. Ho, M.W. Chen, Z.W. Li, Numerical simulation of natural convection of nanofluid in a square enclosure: effects due to uncertainties of viscosity and thermal conductivity, Int. J. Heat Mass Transf. 51 (2008) 4506–4516.

[17] P.M. Congedo, S. Collura, P.M. Congedo, Modeling and analysis of natural convection heat transfer in nanofluids, in: Proceedings of ASME Summer Heat Transfer Conference 3 (2009) 569–579.

[18] B. Ghasemi, S.M. Aminossadati, Natural convection heat transfer in an inclined enclosure filled with a water-Cuo nanofluid, Num. Heat Transf. Part A Appl. 55 (2009) 807–823.

[19] K. Khanafer, K. Vafai, M. Lightstone, Buoyancy-driven heat transfer enhancement in a two dimensional enclosure utilizing nanofluids, Int. J. Heat Mass Transf. 46 (2003) 3639–3653.

[20] J. Kim, Y.T. Kang, C.K. Choi, Analysis of convective instability and heat transfer characteristics of nanofluids, Phys. Fluids 16 (2004) 2395–2401.

[21] A.A. Bakr, Effects of chemical reaction on MHD free convection and mass transfer flow of a micropolar fluid with oscillatory plate velocity and constant heat source in a rotating frame of reference, Commun. Nonlinear Sci. Num. Simul. 16 (2011) 698–710.

[22] K. Das, Effect of chemical reaction and thermal radiation on heat and mass transfer flow of MHD micropolar fluid in a rotating frame of reference, Int. J. Heat Mass Transfer 54 (2011) 3505–3513.

[23] R.K. Tiwari, M.K. Das, Heat transfer augmentation in a two-sided lid-driven differentially heated square cavity utilizing nanofluids, Int. J. Heat Mass Transf. 50 (2007) 2002–2018.

[24] M.A.A. Hamad, I. Pop, Unsteady MHD free convection flow past a vertical permeable flat plate in a rotating frame of reference with constant heat source in a nanofluid, Heat Mass Transf. 7 (2011) 1517–1524.

[25] A. Aziz, A similarity solution for laminar thermal boundary layer over a flat plate with a convective surface boundary condition, Commun. Nonlinear Sci. Num. Simul. 14 (2009) 1064–1068.

[26] O.D. Makinde, A. Aziz, MHD mixed convection from a vertical plate embedded in a porous medium with a convective boundary condition, Int. J. Ther. Sci. 49 (2010) 1813–1820.

[27] A. Ishak, Similarity solutions for flow and heat transfer over a permeable surface with convective boundary condition, Appl. Maths Comput. 217 (2010) 837–842.

[28] N.A. Yacob, A. Ishak, I. Pop, K. Vajravelu, Boundary layer flow past a stretching/shrinking surface beneath an external uniform shear flow with a convective surface boundary condition in a nanofluid, Nanoscale Res. Lett. 6 (2011) 314–319.

[29] N. Liron, H.E. Wilhelm, Integration of the magnetohydrodynamic boundary layer equations by Meksyn's method, J. Comput. Appl. Maths (ZAMM) 54 (1974) 27–37.

[30] R. Ganapathy, A note on oscillatory Couette flow in a rotating system, ASME J. Appl. Mechs. 61 (1994) 208–209.

[31] J. Maxwell, A Treatise on Electricity and Magnetism, second ed., Oxford University Press, Cambridge, UK, 1904.

[32] H.C. Brinkman, Viscosity of concentrated suspensions and solution, J. Chem. Phys. 20 (1952) 571–581.

[33] H.F. Oztop, E. Abu-Nada, Numerical study of natural convection in partially heated rectangular enclosers with nanofluids, Int. J. Heat Fluid Flow 29 (2008) 1326–1336.